MCNPX. To estimate the calculated gamma-ray absorbed dose, data was normalized with the ratio of the measured and calculated data at the position of thyroid in the neck phantom.

3. Results and discussion

From the phantom experiments, it was confirmed that the peak of the thermal neutron flux distribution was at 2 cm depth from the left lateral surface in the head phantom, and the peak value for brain was almost 1.0×10^9 cm^{-2} s^{-1} per proton beam current of 1 mA. The thermal neutron flux of thyroid was 2.8×10^7 cm^{-2} s^{-1} per proton beam current of 1 mA and was much larger than that of the other organs. Because the thyroid was located near the target volume, the influence due to the thermal neutrons produced in brain was larger. In terms of the fast neutrons, ^{115}In(n,n')^{115m}In reaction rate, the value of thyroid was 1.2×10^{-19} s^{-1} atom^{-1} per proton beam current of 1 mA and was more than twice larger than that of other organs. Fig. 4 shows the calculated neutron energy spectrum of lung which is one of the sensitive organs.

The gamma-ray absorbed dose in brain reached the maximum value at 2.7 cm depth from the left lateral surface. The absorbed dose for thyroid was about twice the values for the other organs.

Table 1 shows the calculated-to-measured absorbed dose ratios for thermal and fast neutrons and gamma-ray at the each organ. As a result, the measured thermal and fast neutron absorbed doses were in agreement with the calculated data within the factor of 0.4–2. The discrepancy between the calculated and measured data might be caused by the difference of angular distribution between calculation and experiment.

The estimated uncertainties of the measured thermal and fast neutron flux were 5% and 10%, respectively. The estimated uncertainties of the calculated thermal and fast neutron flux were less than 1%. The measured gamma-ray dose was in good agreement with the calculated data. The estimated uncertainties of the measured and calculated gamma-ray dose were 10% and 1%, respectively. Therefore, it is confirmed that the calculation for gamma-ray can simulate the measurements except in lung. The discrepancy between the calculated and measured gamma-ray doses for lung might be caused by the difference of experimental location of TLD compared with calculation location.

To evaluate the whole body exposure during BNCT medical irradiation, absorbed doses for thermal and fast neutrons were converted to relative biological effectiveness (RBE)-weighted dose. Fig. 5 shows the RBE-weighted dose for each organ. The

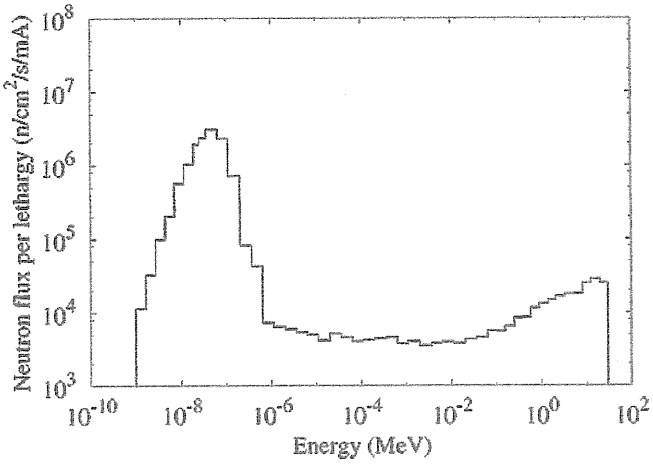

Fig. 4. Calculated neutron energy spectrum at the position of lung.

Table 1
Calculated-to-measured dose ratios for the thermal and fast neutrons and gamma-ray.

Organ	Ratio		
	Thermal neutron	Fast neutron	Gamma-ray
Thyroid	1.72	1.00	1.00
Esophagus	0.66	1.88	0.95
Bone marrow	0.59	1.34	0.96
Lung	1.11	0.89	1.52
Stomach	0.65	1.13	1.00
Liver	0.46	1.21	1.03
Colon	0.52	0.92	1.01
Bladder	0.43	0.86	0.93
Gonad	0.36	0.66	1.06

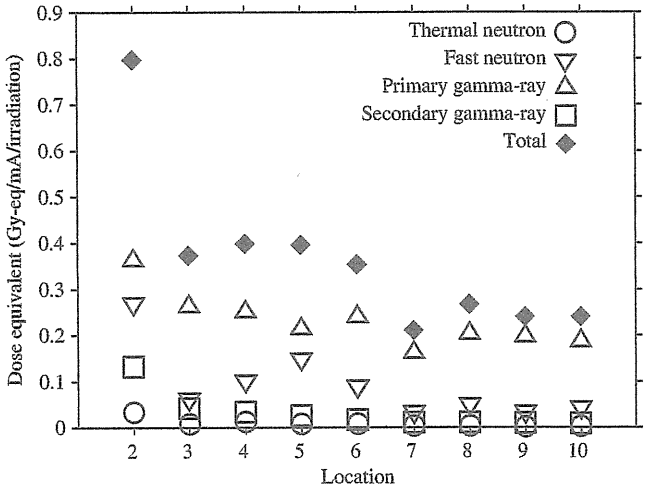

Fig. 5. RBE-weighted doses at locations of 2, thyroid; 3, esophagus; 4, bone marrow; 5, lung; 6, stomach; 7, liver; 8, colon; 9, bladder; and 10, gonad.

irradiation time was assumed 40 min considering typical irradiation. Both of RBEs for thermal and fast neutrons are 3.0, respectively (Tanaka et al., 2009b). It was found that the gamma-ray dose was larger than the other dose components. At the position of thyroid, primary gamma-ray dose accounted for 45% of total dose and fast neutron dose accounted for 34%. And secondary gamma-ray dose accounted for 17% of total dose, because thyroid was located near the target volume with the distance of 13 cm, and thermal neutrons generated at the target was reduced during reaching into thyroid.

On the other hand, at other positions, the total dose of primary gamma-ray and fast neutron accounted for a large fraction of total dose. Hence it is guessed that the whole body exposure can be reduced by shielding the primary gamma-rays generated from the C-BENS components and fast neutrons.

4. Conclusions

The whole body exposure was experimentally evaluated using the activation foils for thermal and fast neutrons and TLDs for gamma-rays. It is confirmed that the calculated MCNPX simulation results for whole body exposure were in agreement with the measured data within the factor of 0.4–2. It was also found that the primary gamma-ray dose and fast neutron dose were main components of the whole body exposure. Based on this research, the additional shields, polyethylene containing LiF and lead plate, were already set outside the aperture in the gap between a

patient and C-BENS to reduce primary gamma-ray and fast neutron dose. The shielding also has halved the thermal neutron fluence and dose.

References

Chadwick, M., Barschall, H., Caswell, R., DeLuca, P., Hale, G., Jones, D., MacFarlane, R., Meulders, J., Schuhmacher, H., Schrewe, U., Wambersie, A., Young, P., 1999. A consistent set of neutron kerma coefficients from thermal to 150 MeV for biologically important materials. Med. Phys. 26 (6), 974–991.

ICRU, 1992. Photon, electron, proton, and neutron interaction data for body tissues, ICRU Report 46, Bethesda, MD.

Sakurai, Y., Kobayashi, T., 2002. The medical-irradiation characteristics for neutron capture therapy at the heavy water neutron irradiation facility of Kyoto University Research Reactor. Med. Phys. 29 (10), 2328–2337.

Tanaka, H., Sakurai, Y., Suzuki, M., Masunaga, S., Kinashi, Y., Kashino, G., Liu, Y., Mitsumoto, T., Yajima, S., Tsutsui, H., Maruhashi, A., Ono, K., 2009a. Characteristics comparison between a cyclotron-based neutron source and KUR-HWNIF for boron neutron capture therapy. Nucl. Instrum. Methods B 267, 1970–1977.

Tanaka, H., Sakurai, Y., Suzuki, M., Takata, T., Masunaga, S., Kinashi, Y., Kashino, G., Liu, Y., Mitsumoto, T., Yajima, S., Tsutsui, H., Takada, M., Maruhashi, A., Ono, K., 2009b. Improvement of dose distribution in phantom by using epithermal neutron source based on the Be(p,n) reaction using a 30 MeV proton cyclotron accelerator. Appl. Radiat. Isot. 67, S258–S261 (13th International congress on neutron capture therapy BNCT: a new option against cancer).

Applied Radiation and Isotopes 69 (2011) 1862–1865

Contents lists available at ScienceDirect

Applied Radiation and Isotopes

journal homepage: www.elsevier.com/locate/apradiso

Study on optimization of multiionization-chamber system for BNCT

T. Fujii [a,*], H. Tanaka [b], A. Maruhashi [b], K. Ono [b], Y. Sakurai [b]

[a] Kyoto University, Graduate School of Engineering, Yoshidahonmachi, sakyo-ku, Kyoto 606-8501, Japan
[b] Research Reactor Institute, Kyoto University, Asashiro-nishi 2-1010, Kumatori-cho, Osaka 590-0494, Japan

ARTICLE INFO

Available online 3 April 2011

Keywords:
Ionization-chamber
Accelerator-based neutron source
Beam monitor

ABSTRACT

In order to monitor stability of doses from the four components such as thermal, epi-thermal, fast neutron and gamma-ray during BNCT irradiation, we are developing a multiionization-chamber system.

This system is consisted of four kinds of ionization chamber, which have specific sensitivity for each component, respectively. Since a suitable structure for each chamber depends on the energy spectrum of the irradiation field, the optimization study of the chamber structures for the epi-thermal neutron beam of cyclotron-based epi-thermal neutron source (C-BENS) was performed by using a Monte Carlo simulation code "PHITS" and suitable chamber-structures were determined.

1. Introduction

In irradiation fields of BNCT, many radiation components such as thermal (−0.5 eV), epi-thermal (0.5 eV–40 keV) and fast (40 keV-) neutron, and gamma-ray exist. Considering that the biological effectiveness of those components are different, accurate evaluation methods at real-time regarding the doses from 4-components have to be established for the quality assurance of BNCT. Based on this background, we suggested a "multiionization-chamber system" to monitor the stability of doses from the 4-components at real time during the irradiation. In this system, four kinds of ionization chambers (IC) having specific response for each component, are used in current mode. They are preferred to be small enough to have negligible effect on the beam, when placed at the edge of the beam collimator in the BNCT facility.

To complete this system, the structural optimizations of each IC for wall material, wall thickness and gas, are necessary for every irradiation fields. In this paper, the optimization study for the epi-thermal neutron spectrum of the cyclotron-based epi-thermal neutron source (C-BENS) in Kyoto University Research Reactor Institute (KURRI) is reported.

2. Material and methods

The optimization study was performed by using a Monte Carlo simulation code PHITS "Particle Heavy Ion Transport code System". This code can treat all ion transports and their deposit energy distribution (Iwase and Niita, 2002). The ionization chambers were modeled based on 2cc-chamber of the IC-17 series manufactured by Far West Technology (FWT). Combinations of each IC considered in this study is shown in Table 1.

For the IC of gamma-ray component (Gamma-IC), the surveys were performed for wall materials such as graphite (G), magnesium (Mg) and aluminum (Al), and gases such as argon (Ar) and carbon dioxide (CO_2). For the IC of thermal component in neutron (Thermal-IC), the surveys were performed for silicon nitride wall (Si_3N_4) and nitrogen gas (N_2) to enhance thermal response via $^{14}N(n,p)$ reaction. For the IC of epi-thermal component (Epi-IC), polyethylene wall (Poly) was selected as the effective moderator from epi-thermal to thermal, and N_2 gas was selected in the same way as on Thermal-IC. In addition, the sensitization in case that ^{10}B is coated at 1.8 μm thickness on inner wall was investigated for Epi-IC. For the IC of fast component (Fast-IC), Poly wall and methane gas (CH_4) were selected to enhance fast response via recoil proton generated in wall and gas.

The optimization surveys for wall thickness were performed from 0 to 10 mm in 1 mm increment, for Gamma-IC, Thermal-IC, and Fast-IC. As for Epi-IC, the survey was performed from 0 to 100 mm in 10 mm increment to confirm the thermalization of epi-thermal neutron in Poly-wall. The IC responses were evaluated as the electric-currents (hereinafter called the current) generated from respective components.

In the PHITS-simulation, all ICs were handled in the same manner. The energy deposited in gas by charged particle (proton, electron, alpha etc.) is calculated with a tally called Deposit Tally [T-deposit]. The unit of output obtained in a tally is MeV/cm^3, which can be converted into number of electron-ion pairs by using the gas volume in the chamber and its W-value for mainly generated-particles needed to create such a pair (ICRU, 1979).

* Corresponding author. Tel./fax: +81 72 451 2604.
E-mail address: f.takaaki@ft7.ecs.kyoto-u.ac.jp (T. Fujii).

0969-8043/$ - see front matter © 2011 Elsevier Ltd. All rights reserved.
doi:10.1016/j.apradiso.2011.03.031

Table 1
Combinations of ionization chamber.

IC-type	Wall (Gas)	Wall thickness (mm) (Increment (mm))
Gamma-IC	G/Mg/Al (Ar/CO_2)	0–10 (1)
Thermal-IC	$Si_3N_4(N_2)$	0–10 (1)
Epi-IC	$Poly(N_2)+^{10}B$	0–100 (10)
Fast-IC	$Poly(CH_4)$	0–10 (1)

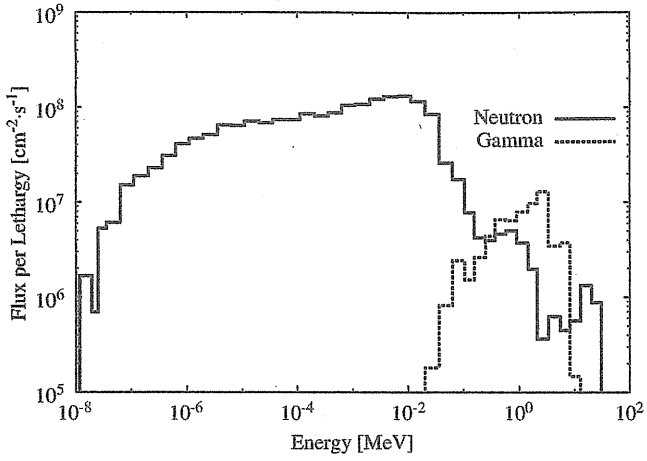

Fig. 1. Energy spectra of epi-thermal neutron beam (solid line: neutron and dash line: gamma-ray).

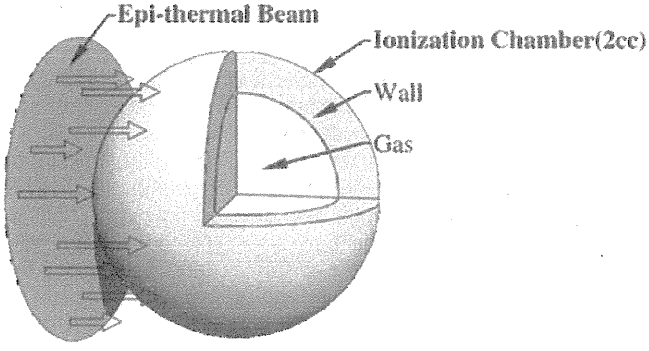

Fig. 2. Geometry in PHITS calculation.

The number of electron per second, namely current, is finally obtained using the beam intensity and the elementary charge in gas. The energy spectrum data obtained at the collimator aperture of C-BENS (Tanaka and Sakurai, 2009) were set as the source data of neutron and gamma-ray. The energy spectra of the epi-thermal neutron beam at C-BENS used in this study are shown in Fig. 1 (solid line: neutron and dash line: gamma-ray). The neutron spectrum was divided into three components (thermal, epi-thermal and fast), and each component was used as a neutron source for its energy range. The geometry used in the PHITS is shown in Fig. 2. A chamber is placed facing with the surface source for gamma-ray and neutron from C-BENS. The directionality of the source is assumed to be parallel. The diameter of the surface source is the same as that of the chamber outside-wall in order to reduce the calculation time.

3. Simulation results

The calculated currents for all ICs were in the pA-level, which is a sufficiently measurable level using an ammeter.

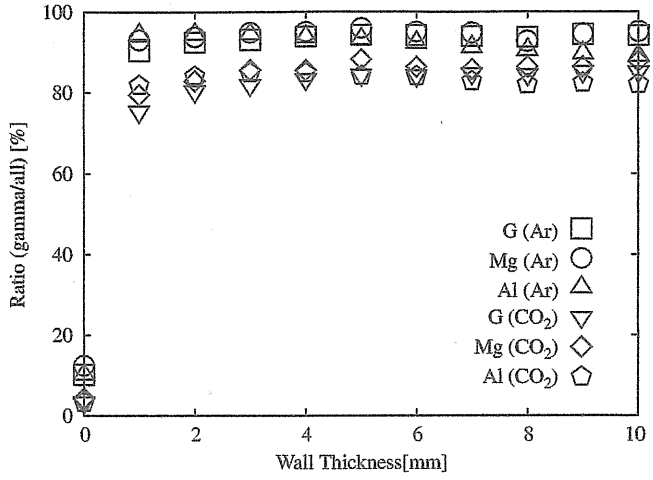

Fig. 3. The relationship between gamma-ray ratio and wall thickness.

3.1. Gamma-IC

Chambers filled with argon gas showed higher sensitivity ratio than that of CO_2 gas for gamma component by 20%, since deposited energy from charged particles produced by reaction with fast component is suppressed by the low cross section in argon.

This shows that a Graphite wall of 4-mm thickness and argon gas is the best combination in the three wall materials. The ratio of gamma-ray to all components is approximately 95% in the electric current using this combination (see Fig. 3.)

3.2. Thermal-IC

It is difficult to obtain a higher current compared to the other three components. Because, there is low thermal component at C-BENS originally (see Fig. 4(a)). The ratio of thermal to all components did not depend on the wall thickness but mainly depend on gas type. So the optimum thickness of Si_3N_4 wall is between 1 and 10 mm in terms of this study, and the ratio of thermal to all components at these thicknesses is approximately 20%.

3.3. Epi-IC

The 30 mm thick of Poly generates the peak electric-current for epi-thermal component due to the reaction with N_2 gas and neutron moderated in wall, and the ^{10}B-coated chamber generates two order higher current than the no-coated one due to the large energy-transfer by alpha and lithium particle from $^{10}B(n, \alpha)^7Li$ reaction (see Fig. 4(b)). This means that the wall also plays a role as epi-thermal moderator, and the thermalized epi-thermal component reacts with the coating ^{10}B and the N_2 gas. The ratio of epi-thermal to all components at 30 mm is approximately 96%.

3.4. Fast-IC

The current derived from epi-thermal component is dominant in smaller wall thickness, and it decreases with increases in wall thickness (see Fig. 4(c)). The ratio of fast to all components at 10 mm is approximately 50%.

4. Experimental results

Experiments were performed at the C-BENS facility to verify the PHITS simulations and currents calculation methods. As the

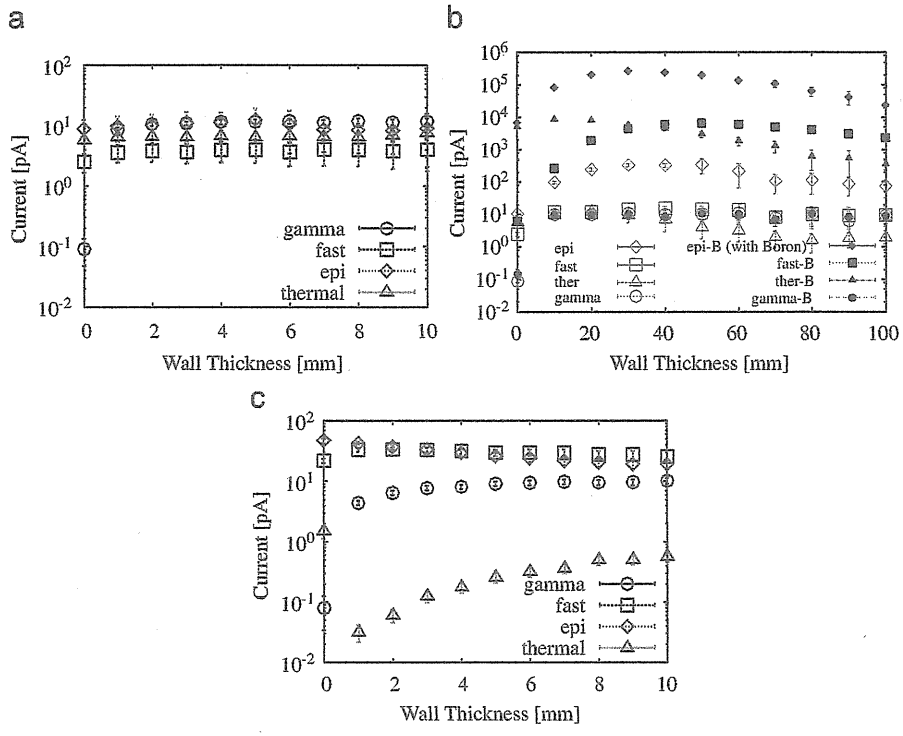

Fig. 4. Comparison of current for each neutron chamber: (a) thermal-IC, (b) epi-IC, and (c) fast-IC.

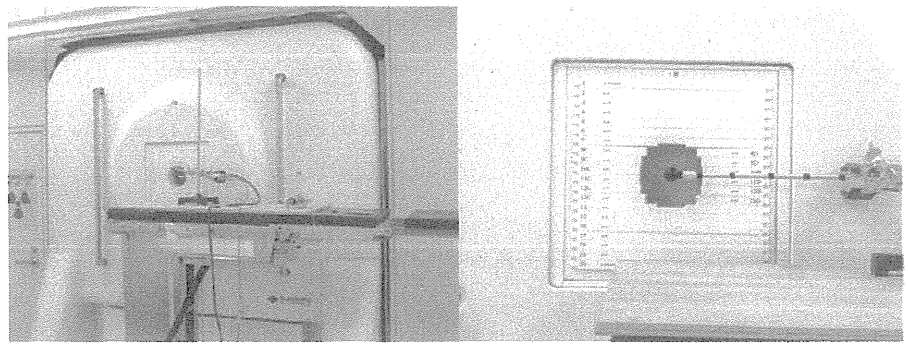

Fig. 5. Experimental settings for the ionization chambers at C-BENS.

Table 2
Comparison for the obtained currents at C-BENS between the experiments and PHITS-simulations.

IC-type	PHITS (pA)	Exp (pA)	PHITS/Exp
Fast-IC (1cc)	26.6 ± 2.0	28 ± 2	0.95 ± 0.15
Gamma-IC (2cc)	30.1 ± 2.5	42 ± 3	0.71 ± 0.13

Gamma-IC and Fast-IC, commercially available chambers (IC-17G(2cc) and IC-17P(1cc) manufactured by FWT) were used. Fig. 5 shows the experimental settings at the C-BENS facility. The ionization chambers were placed at the center of the epi-thermal beam collimator (Fig. 5). Neutron beam spectrum is the same configuration of the simulation source.

Table 2 shows the results of current comparison between experiments and calculation using PHITS. The experiment and the simulation results were in good agreement for Fast-IC chambers within 5%. For Gamma-IC, however, calculation showed 30% disagreement compared with experiments. The differences between calculation and experiment seems to derive from charge estimation methods or gamma-ray data we used.

5. Conclusions

The optimization surveys for wall and gas of ICs using multi-ionization chamber system were performed for the C-BENS facility. For Gamma-IC, it is concluded that graphite wall of 4 mm thickness and argon gas is the best combination. The ratio of gamma-ray to all components is approximately 95% using this combination.

For Thermal-IC, the optimum thickness of IC wall is 1–10 mm of Si_3N_4 in terms of this study due to independence from wall thickness. The ratio of thermal to all components at these thicknesses is approximately 20%. For Epi-IC, 30 mm of Poly generates the peak of current for epi-thermal component. But, this size of Poly increases thermal component at 9% in the

neutron beam when the IC is placed at the edge of the collimator aperture for the C-BENS side. The optimum thickness of Poly was determined to 10 mm in this study, because the ratio of epithermal to all components is large (approximately 90%) enough to get the sufficient current and the increase of thermal components is negligible by the Poly of this thickness. For Fast-IC, the optimum thickness of Poly-wall is 10 mm, and the ratio of fast to all components is approximately 50%.

As works in the near future, response factors for 4-components of 4-ICs have to be determined, respectively, based on experimental results from several fields having different neutron spectra, and we will finally make the optimized-ICs and complete the multiionization-chamber system for C-BENS.

References

ICRU, 1979. Average energy required to produce an ion pair. ICRU Report 31, Bethesdas, MD.

Iwase, H., Niita, K., 2002. Development of general-purpose particle and heavy ion transport Monte Carlo code. J. Nucl. Sci. Technol. 39 (11), 1142–1151.

Tanaka, H., Sakurai, Y., 2009. Improvement of dose distribution in phantom by using epithermal neutron source based on the Be(p,n) reaction using a 30 MeV proton cyclotron accelerator. Appl. Radiat. Isotop. 67, 258–261.